

Flexible Conductive Polymer Patterns from Vapor Polymerizable and Photo-Cross-Linkable EDOT

Jeonghun Kim, Jungmok You, and Eunkyong Kim*

Department of Chemical and Biomolecular Engineering, Yonsei University 262 Seongsanno, Seodaemun-gu, Seoul 120-749, Korea

Received November 16, 2009; Revised Manuscript Received January 25, 2010

ABSTRACT: We explored direct photopatterning of a vapor polymerizable and photo-cross-linkable 3,4-ethylenedioxythiophene (EDOT) to make it suitable for use in electronics applications. We prepared a conductive polymer, PEDOT-MA, using vapor phase polymerization (VPP) of the (2,3-dihydrothieno-[3,4-*b*][1,4]dioxin-2-yl)methyl methacrylate (EDOT-MA) and photochemically induced a conductivity change of the PEDOT-MA film to ensure a flexible conductive pattern. The room-temperature conductivity (σ_{RT}) of the PEDOT-MA film on PET was 30–120 S/cm, depending on the oxidant layer thickness and was increased $\sim 30\%$ when the PEDOT-MA film was doped with aqueous solution of *p*-toluenesulfonic acid. Photoreaction of PEDOT-MA decreased the σ_{RT} to 1.7×10^{-3} S/cm because of the photo-cross-linking of the side chain. The transparency of the conductive films was tuned using the vapor polymerization time to control the film thickness. The photo-cross-linking reaction of the side chain generated micropatterns having line widths of 50–0.9 μm , in which the light-exposed areas appeared as bleached and less conductive. A diffractive, flexible, conductive film with 41% of diffraction efficiency was obtained from the line-patterned film having a spacing of 0.9 μm .

Introduction

The combination of high electrical conductivity and transparency in conducting polymers continues to advance applications, including flexible displays,¹ transistors,^{2a} biosensors, region-specific cell growth,^{2b} photovoltaic cells,³ and protein fixation.⁴ In such applications, patterning of the conductive polymer (CP) is a key prerequisite, and thus considerable efforts have been made to pattern CPs using top-down and bottom-up methods including plasma etching, micromolding, photolithography, printing techniques, self-assembly of block copolymers, and instability-induced patterning.⁵ These methods allow for control over the pattern resolution and conductivity, so they are highly valuable processes for micro- and nanotechnological applications.

In particular, the direct photopatterning of polythiophenes has been extensively researched with the view to their simple and dry process. Films of poly(3-alkylthiophenes) (P3ATs) undergo photo-cross-linking, become insoluble after UV irradiation,⁶ and are initiated by the hydrogen abstraction reaction of alkyl side chains.⁷ Direct patterning of P3ATs can also be achieved through exposure to an electron beam⁸ to generate lines up to 50 nm wide. These direct photopatternings require high intensity incident light, which inevitably leads to photo-oxidation of the polymer. Therefore, P3ATs have been designed to be more photosensitive by the attachment of photoreactive acrylic moieties,⁹ cinnamoyl groups,¹⁰ bis-arylazide groups,¹¹ and pendant tetrahydropyranyl (THP) groups.¹²

Compared with polythiophenes with an acrylic group, poly(ethylenedioxythiophenes) (PEDOTs) bearing a pendant acrylate group have been known to be more stable during photopatterning processes, and they undergo selective photo-cross-linking of the acrylate group without photodecomposition of the parent

thiophene ring.¹³ This process is useful for photolithographic patterning where the soluble PEDOT substituted with a pendant acrylate group becomes insoluble after the photoreaction and remains as a conductive pattern after a wet etching process.

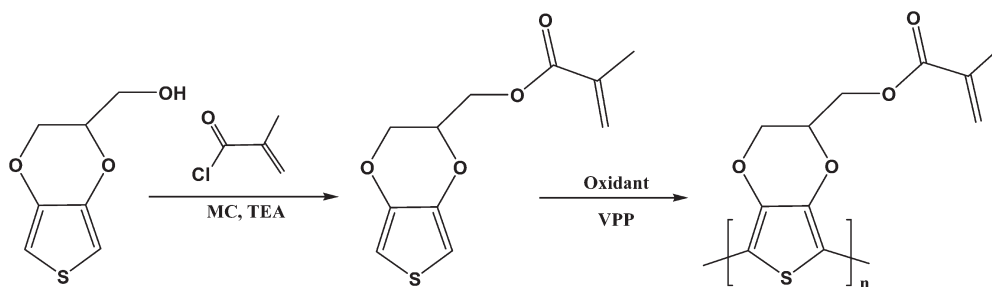
In our previous study, we reported a direct photopatterning method using a PEDOT-bearing alkyl methacrylate side group.¹⁴ The working principle in this patterning was based on twisting of the conductive PEDOT channel through photo-cross-linking of the side-chain methacrylate group. This method afforded direct patterns without the need for a wet etching process. However, the substrate for the polymer film deposition has to be conductive when the polymer is electrochemically deposited. In this context, an ethylenedioxythiophene (EDOT) derivative having a short methacrylate group is challenging because it could be deposited using vapor phase polymerization (VPP). The VPP method generally affords PEDOT films with high film uniformity on any substrate including insulative substrates.¹⁵ Herein we report the synthesis and polymerization of an EDOT bearing a short methacrylate side group and examine the deposition and photopatternability of the CP film.

Experimental Section

Materials. 3,4-Dimethoxythiophene, 3-chloro-1,2-propanediol, *p*-toluenesulfonic acid monohydrate, anhydrous toluene, anhydrous dimethylformamide, anhydrous methylene chloride, methacryloyl chloride, triethylamine, iron(III) *p*-toluenesulfonate, anhydrous isopropylalcohol, lithium perchlorate, and potassium carbonate were purchased from Aldrich Chemicals and used without further purification. The photoinitiator, irgacure 184, was purchased from Ciba Specialty Chemicals. Thieno[3,4-*b*]-1,4-dioxin-2-methanol (EDOT-MOH) was synthesized as previously described. Polyethylene terephthalate (PET) film and ITO (conductivity = 100 Ω/sq) were purchased from Kolon (Korea) and Aldrich, respectively.

*Corresponding author. E-mail: eunkim@yonsei.kr.

Scheme 1. Synthesis of EDOT-MA and Polymerization of EDOT-MA



Instruments. The ^1H NMR spectrum was obtained using the BRUKER ARX-400 spectrometer. The absorbance and transmittance of the polymer (PEDOT-MA) coatings on the substrates (glass or 0.5 mm thick PET film) were characterized using an AvaSpec spectrometer (AvaSpec-2048; light source: Ava-Light-DHS). The FT-IR spectra were obtained using a TENSOR 37 apparatus (Bruker). To measure the FT-IR during the photoreaction, the oxidant solution was spin coated onto a KBr pellet, and a CP was directly deposited onto the pellet using the VPP method. The PEDOT- or PEDOT-MA-coated pellet was loaded onto the sample holder and characterized before UV irradiation. The PEDOT- or PEDOT-MA-coated pellet was coated with a solution of irgacure 184 (0.3 M) in ethanol and then exposed to UV source for 5 min (9 J/cm^2). These KBr pellets were washed with ethanol to remove excess irgacure 184 and characterized with FT-IR. The morphology of the polymer was measured with atomic force microscopy (AFM, dimension 3100 SPM equipped with a Nanoscope IV devised by Digital Instruments from Santa Barbara, CA) and a field emission scanning electron microscope (FE-SEM, Hitachi, model S-4200). The PEDOT-MA was coated onto an Si wafer using VPP to examine the morphologies using AFM and SEM. The patterns in the CP films were examined using optical microscopy (BX-51, Olympus) and a digital camera (model: Canon Power Shot A640). The conductivities of the samples were measured using electrochemical analyzer (CH Instruments, CHI624B) and a four-point probe (ALS, Japan). The probe was equipped with four spring-loaded tungsten carbide needles spaced 1 mm apart. To eliminate errors from thermovoltages and voltmeter offsets, two current pulses with opposite signs were used for each measurement point.

Synthesis of Methacrylate-Functionalized EDOT (EDOT-MA). The solution of EDOT-OH (5.8 mmol) in methylene chloride (30 mL) was added to a flask equipped with N_2 purge. After the addition of triethylamine (5.8 mmol) at 0°C , the mixture was stirred for 20 min, and then methacryloyl chloride (5.8 mmol) was dropped for 10 min under a N_2 atmosphere. After 24 h of stirring at RT, the resulting mixture was washed with 1 M HCl (aq) and extracted with methylene chloride. The organic layer was washed with water, and the organic phase was dried with MgSO_4 . After removal of the solvent, remaining crude product was isolated by column chromatography with silica (hexane/ethylacetate 2:1) to give EDOT-MA as a viscous yellow liquid (yield 93%). ^1H NMR (400 MHz, CDCl_3 , δ): 6.36 (m, 2H, Th), 6.16–5.57 (m, 2H, $\text{C}=\text{CH}_2$), 4.42–4.34 (m, 3H, $-\text{OCH}_2\text{CH}-$), 4.27–4.05 (m, 2H, $\text{O}=\text{C}-\text{OCH}_2-$), 1.95 (s, 3H, $-\text{CH}_3$). FT-IR (neat, cm^{-1}): 2958, 1716, 1637, 1483, 1450, 1427, 1377, 1296, 1184, 1062, 1016, 947, 921, 848. Anal. Calcd for $\text{C}_{11}\text{H}_{12}\text{O}_4\text{S}$: C, 54.99; H, 5.03; O, 26.64; S, 13.35. Found: C, 54.89; H, 5.33; O, 27.04; S, 12.74%.

Vapor Phase Polymerization. VPP of the EDOT-MA was performed in a glass chamber equipped with a heating plate. The chamber was flushed with nitrogen before the polymerization, and the heater was used to raise the temperature of the monomer reservoir to vaporize the monomer. The chamber was filled with EDOT-MA vapor by heating the EDOT-MA reservoir to 90°C right before the substrate transfer. A PET film was used as the

flexible substrate. The substrate was coated with Fe(III) tosylate as the oxidant using oxidant solution which consists of the oxidant (0.06, 0.20, or 0.40 M), isopropyl alcohol (5 mL), and pyridine (0.031 g, 0.4 mmol) under a dry atmosphere. After the solution was spin coated, the substrates were dried at 60°C to give oxidant layers having different thickness according to the concentration of Fe(III) tosylate. Then, the oxidant-coated substrates were transferred to the glass chamber, which was filled with the EDOT-MA vapor for the VPP. After 1 h, the PEDOT-MA-coated substrates were washed with ethanol and distilled water and then dried under nitrogen. The PEDOT-MA films were deposited with film thickness of 30, 70, and 260 nm from the oxidant layers coated with the Fe(III) tosylate concentration of 0.06, 0.20, or 0.40 M, respectively. The σ_{RT} values of the PEDOT-MA films were 30 ± 10 , 120 ± 30 , and $45 \pm 2\text{ S/cm}$, respectively. The substrate was either PET or a slide glass for bending or doping experiment, respectively. The σ_{RT} of the PEDOT-MA film ($130 \pm 27\text{ S/cm}$) on a glass, prepared from the oxidant concentration of 0.20 M, was increased to $178 \pm 20\text{ S/cm}$ when the film was doped with aqueous solution of *p*-toluenesulfonic acid (1 M) for 10 min.

Conductive Polymer Patterning. Photopatterning was carried out using a UV light source (PowerArc UV100, 13.05 mW/cm^2) and a photomask coated with Cr on quartz. The coated CP on a nonconductive substrate such as a slide glass or flexible PET film was coated with a 0.5 wt % initiator solution of Irgacure 184 dissolved in an anhydrous organic solvent (ethanol or diethyl ether) for a fast and efficient photoreaction of the methacrylate group and was then placed under the photomask. The CP film was irradiated, and then the initiator was washed with fresh ethanol. The irradiated area was bleached and showed patterns. The mask pattern size was varied from 0.5 to $100\text{ }\mu\text{m}$, but the pattern resolution was limited to $0.9\text{ }\mu\text{m}$. The energy density was varied from 0.1 to 90 J cm^{-2} in the plane of the film. Patterns with $< 5\text{ }\mu\text{m}$ line spacing showed diffraction of light. The grating from the line pattern was read in self-diffraction mode.

Results and Discussion

Optical and Electrical Properties of PEDOT-MA on Flexible Substrate. Scheme 1 shows a synthesis of EDOT-MA with EDOT-OH¹⁶ and polymerization of EDOT-MA to PEDOT-MA. A photopolymerizable EDOT with a methacrylate group (EDOT-MA) was synthesized from thieno[3,4-*b*]-1,4-dioxin-2-methanol (EDOT-OH) and methacryloyl chloride using the previously described method with slight modifications.¹⁴ The EDOT-MA was polymerized using VPP to form a patternable CP film on a flexible PET substrate. In the polymerization, the monomer was vaporized at 90°C , which was a higher temperature than that used for the VPP of the EDOT¹⁵ because of the higher molecular weight of the EDOT-MA. The PEDOT-MA films on the glass and PET substrate were homogeneous without defects and could be coated onto a large area of a PET film (450 cm^2), as shown in Figure 1a,b. The thickness of the PEDOT-MA film on the substrate was 40–200 nm and was controlled by the vapor polymerization time.

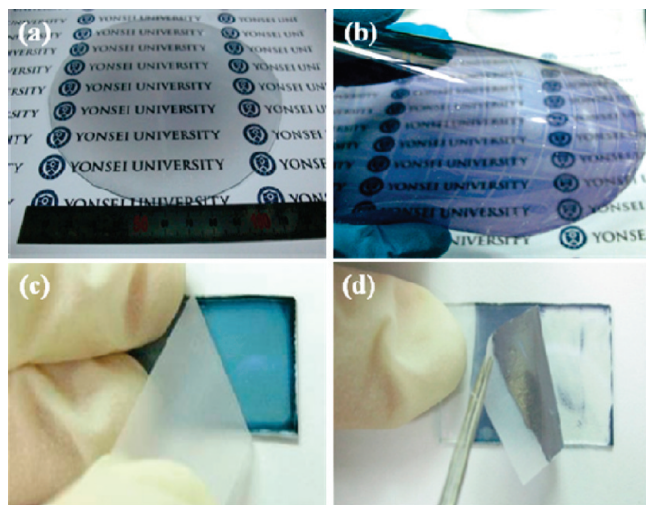


Figure 1. Photographs of the PEDOT-MA film on a PET film (a) before and (b) after photopatterning. Adhesion test of the PEDOT-MA film (c) prepared by VPP and (d) prepared by electrochemical method on ITO glass.

The PEDOT-MA film from the VPP (thickness: 40 nm) showed an absorption maximum near 550 nm with a transparency of 68% in the visible range. It showed good adhesion to the flexible PET and ITO glasses, as determined using the tape test. The adhesion of the PEDOT-MA film on a glass substrate (Figure 1c) was strong without detachment and significantly enhanced compared with that of the electrochemically deposited film (Figure 1d).

The PEDOT-MA film on PET prepared on a thin oxidant layer, coated from a dilute Fe(III) tosylate concentration (0.06 M), showed σ_{RT} of ~ 30 S/cm, which was lower than that for VPP-PEDOT.¹⁵ The σ_{RT} was increased to 120 S/cm when the film was prepared on an oxidant layer that was coated from a concentrated solution of Fe(III) tosylate (0.20 M). This could be attributed to doping of PEDOT-MA from the oxidant. However, σ_{RT} of the film was decreased to 45 S/cm when the oxidant layer contained high Fe(III) tosylate, possibly because of the formation of aggregates originating from the excess oxidant. The σ_{RT} of the PEDOT-MA film (70 nm) on a slide glass was increased from 135 to 178 S/cm when the PEDOT-MA film was additionally doped with aqueous *p*-toluenesulfonic acid. The conductivity of PEDOT-MA is not very high but sufficient for use as a conductive surface in many applications.¹⁷ For the patterning and bending experiment, we used the film having σ_{RT} of 30 S/cm, unless specified.

The flexibility of the PEDOT-MA film (thickness of 100 nm) on PET at different bending levels was determined by measuring the resistivities at four fixed points at different bending angles or radius.¹⁸ To compare, we prepared a PEDOT film on PET by VPP with the same thickness as that of the PEDOT-MA film (100 nm).

Figure 2a shows the room-temperature resistivities (γ_{RT}) when the PEDOT-MA film was bent. Interestingly, the γ_{RT} did not increase much ($\sim 10\%$) when the film was bent with a bending angle (θ) of 80° or a bending radius (r) of 0.65 cm. The resistivity increase reached 30% when the bending was more severe with a bending radius of 0.4 cm ($\theta = 40^\circ$). Surprisingly, the resistivity increase by bending of the PEDOT-MA film was smaller than that of the PEDOT film by VPP ($\sigma_{RT} = 125$ S/cm) when both films were bent with the bending angle (θ) of 120° – 80° . In addition, compared with the well-known ITO-coated PET film,¹⁸ the conductivity loss due to bending of the PEDOT-MA film was much smaller

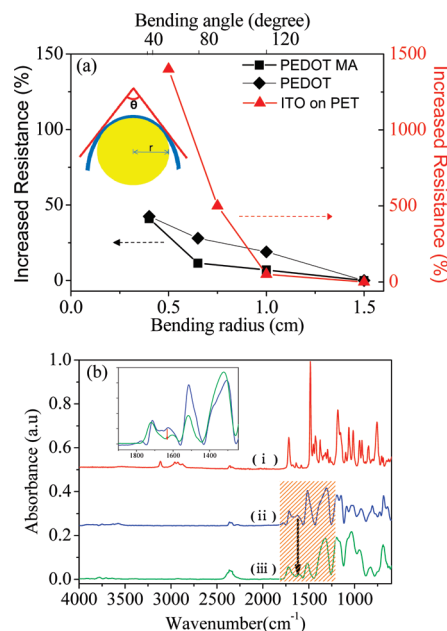


Figure 2. (a) γ_{RT} of PEDOT-MA, PEDOT, and ITO on PET according to r and θ . The thickness of conductive polymer films was ~ 100 nm. (b) FT-IR spectra of (i) the monomer, (ii) vapor polymerized PEDOT-MA on KBr pellet, and (iii) UV exposed PEDOT-MA film on KBr pellet using UV light. Inset: magnitude spectrum of marked region with orange line.

for the same r . The threshold r for drastic conductivity change was 0.4 and > 1 cm for the PEDOT-MA and the ITO on the PET film, respectively, indicating that the PEDOT-MA film has more flexibility in conductivity.

The morphology of the PEDOT-MA films before and after bending was characterized using an AFM. As shown in Figure S2 of the Supporting Information, there was not much change in morphology at bending point before and after bending of the CP on PET film, even with a large bending angle of 30° . The mean roughness values of PEDOT-MA before and after bending were 8.39 and 8.40 nm, respectively. This indicates that PEDOT-MA has good stability for bending.

After we prepared the PEDOT-MA film using VPP and established its adhesion and conductivity, we examined the side chain reactivity of the PEDOT-MA for photopatterning purposes. Thin films of PEDOT-MA cross-linked successfully within a few minutes of UV irradiation. Absorption in the visible region decreased significantly upon UV exposure of the film. Because the visible bands are responsible for the electronic conduction in the PEDOT main chain, the spectral change indicates that the conduction paths were broken.

FT-IR Study of Photo-Cross-Linking and Conductivity Changes from UV Irradiation. The IR absorption was changed when the films were deposited and subsequently exposed to UV, indicating that the intensity for the methacrylate decreases during photoirradiation (Figure 2b). The peak at 3115 cm^{-1} for monomer (Figure 2b(i)) was due to the 2,5-hydrogen atoms on the thiophene ring.¹⁹ The peak at 3115 cm^{-1} disappeared in the polymerized sample (dashed line). This result confirms the polymerization at the thiophene ring due to the use of the VPP method. The C=C stretching vibration frequency of the methacrylate transition²⁰ at 1637 cm^{-1} of the PEDOT-MA appeared in a similar region as it did for the monomer, indicating that the methacrylate groups remained intact during the VPP at 90°C . The peaks at $\sim 2950\text{ cm}^{-1}$ can be attributed to the vibrational frequency of the C-H stretching of the methacrylates^{21,22} and changed

little after polymerization. The C=O vibration frequency for the ester group appeared as a large peak at 1716 cm^{-1} in all three samples, with no detectable change in intensity or position.

The C=C stretching vibration frequency of the methacrylates decreased significantly after UV exposure (9 J/cm^2) compared with that of the unexposed PEDOT-MA in Figure 2b (ii). The photochemical decrease in areal intensity of the UV exposed film (Figure 2b (iii)) was determined to be $\sim 51\%$ compared with that of the unexposed PEDOT-MA film. This decrease is a direct proof of the photopolymerization of the methacrylate groups. Therefore, the observed spectral change confirmed that the thiophene rings were polymerized using the VPP method in the first step (Figure 2b (ii)) and that the methacrylates were polymerized photochemically (Figure 2b (iii)).

It was noteworthy that the IR intensity for the thiophene unit²⁴ at 1520 cm^{-1} was also decreased to $\sim 54\%$ after UV exposure with a dose of 9 J/cm^2 . This indicates that the conjugation through thiophene main chain is broken by the photoreaction. Indeed, the σ_{RT} of the PEDOT-MA film (30 S/cm) was decreased to 12.7 and 0.98 S/cm for UV dose of 3.9 and 19.5 J/cm^2 , corresponding to the conductivity loss of 55.6 and 96.6% , respectively. The direct photodecomposition for thiophene unit requires higher energy than the photo-cross-linking reaction of the methacrylates.²³ The thiophene can be oxidized and lose conductivity under a high dose of UV irradiation in air. To examine the origin of the conductivity loss by the photoreaction, the σ_{RT} of PEDOT film was compared with that of the PEDOT-MA film upon UV irradiation. The PEDOT and PEDOT coated with initiator were irradiated under the same dose of UV as that of PEDOT-MA film. The conductivities of the film of PEDOT and PEDOT coated with initiator were reduced to be 6.8 and 15.8% by 3.9 J/cm^2 , respectively, which were much smaller than the conductivity loss of PEDOT-MA film with the same dose. In addition, the FT-IR spectra of the film of PEDOT coated with initiator did not show any change in the intensity for the C=C conjugation of the thiophene part, (C=C)_{Th} (Figure S1 in the Supporting Information). Therefore, the photoinduced conductivity loss in PEDOT-MA film could be ascribed to the photo-cross-linking of the methacrylate unit at the side chain, which possibly leads to twisting or bending of the main chain. Figure 3a shows the effect of light exposure on the conductivity of the PEDOT-MA film having σ_{RT} of 30 S/cm . The conductivity decay was well correlated to the first exponential decay curve according to eq 1

$$\sigma_t/\sigma_0 = 0.917 \exp(-D/5.29) + 0.066 \quad (1)$$

where σ_0 and σ_t are the conductivity of the film before and after irradiation with a light dose ($D, \text{J/cm}^2$), respectively.

Similarly, the *p*-toluenesulfonic-acid-doped PEDOT-MA (70 nm) film showed a dramatic decrease in σ_{RT} from 178 to 0.055 S/cm upon exposure to a UV source, as shown in Figure 3a. The σ_{RT} of the UV exposed film was slightly increased from 0.055 to 0.092 S/cm upon *p*-toluenesulfonic acid doping. This result indicates that doping is not effective for the conductivity change of the photo-cross-linked polymers. In addition, we may conclude that the effect of the local gradient of dopant concentration on the conductivity change by UV exposure may be small.

Morphology Changes of PEDOT-MA Due to Photo-Cross-Linking. The morphology of the PEDOT-MA films before and after UV irradiation was characterized using an AFM and a scanning electron microscope (SEM). Figure 4a,b

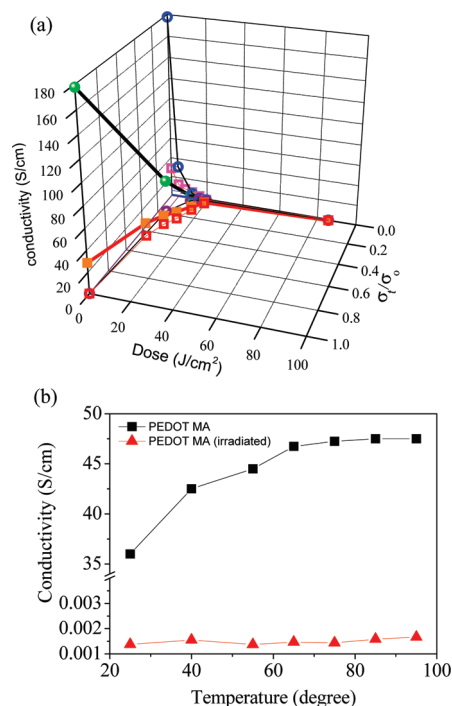


Figure 3. (a) Conductivity change according to UV dose for the PEDOT-MA films having σ_{RT} of 30 (orange square with red line) and 178 S/cm (green circle with black line). The 2D projections are shown as empty symbols for films having σ_{RT} of 30 (square) and 178 S/cm (circle). (b) Plot of the conductivity versus temperature of the PEDOT-MA film before (black) and after UV exposure (red) with a dose of 90 J/cm^2 .

shows the AFM images of the PEDOT-MA coated onto a silicon wafer using the VPP method before and after UV irradiation. Before UV irradiation, the coated CP film showed a smooth morphology, but after UV irradiation, the surface became rough. The roughness values of the film were 13.48 and 23.54 nm for the PEDOT-MA film before and after UV exposure for 20 min , respectively. Also, in the SEM images shown in Figure 4c,d, the original conductive film before UV irradiation had a smooth surface, but after irradiation, the film showed congregated flocks with pores, possibly because of shrinkage by the photo-cross-linking of the methacrylate group on the PEDOT side chain. The surface morphology changes from the photoirradiation of the PEDOT-MA film due to the side-chain cross-linking could lead to main chain distortion and volume shrinkage. Accordingly, interchain interaction of the polymers should be decreased to deter charge-transport among the conductive PEDOT chains because of the side chain cross-linking. Therefore, the photopolymerization at the side chain forced structural changes in the thiophene main chain to covalently bond the methacrylate units in the polymer or between the polymer rods to produce less-conductive structures. As Figure 3b (triangle) shows, the conductivity of the UV exposed film (for 1 h) was almost invariant over the temperature range, whereas the conductivity of the unexposed film was increased as the temperature was elevated. This result could be ascribed to the shrinkage and distortion of the PEDOT main chain from the side chain photo-cross-linking, which breaks the electronic conjugation.

Small conductivity changes have been reported after the photo-cross-linking of poly-3-alkylthiophene with a photoreactive side chain.²³ However, in PEDOT-MA, the content of the photoreactive side chain is much larger than that of poly-3-alkylthiophene, and thus the cross-linking of the side

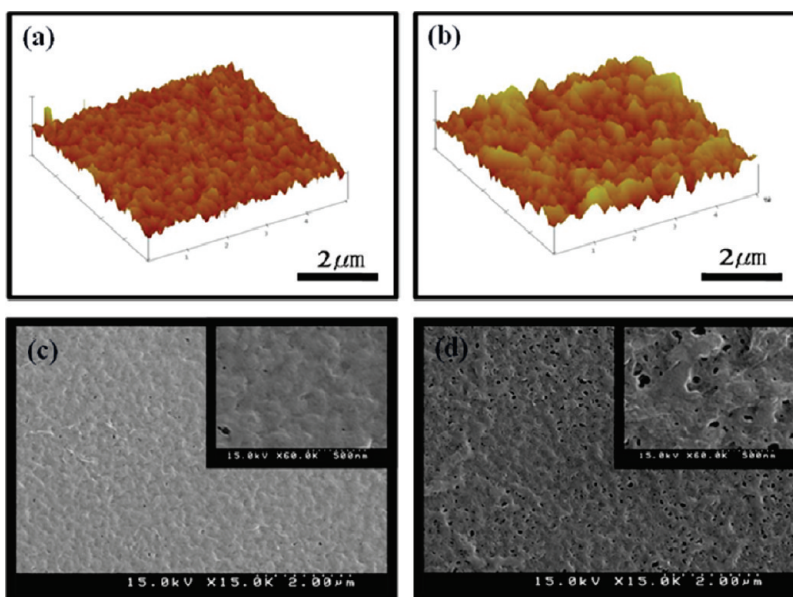


Figure 4. AFM images of PEDOT-MA film by VPP (a) before and (b) after photoirradiation. FE-SEM images of PEDOT-MA film by VPP (c) before and (d) after photoirradiation. Insets show the magnified images.

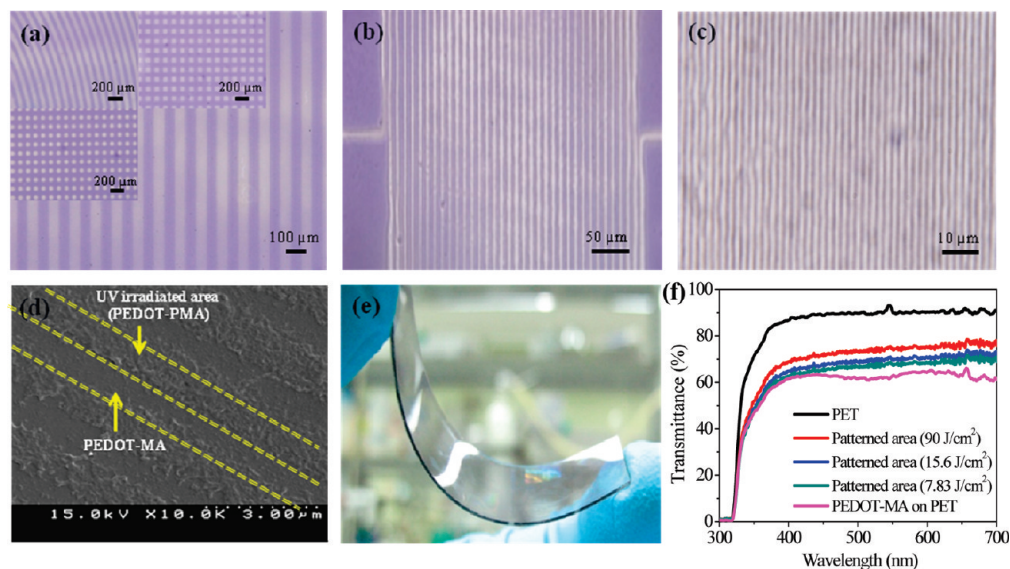


Figure 5. Optical microscopic images of the PEDOT-MA film with pattern size of (a) 50 μm (insets show various patterns with different line widths), (b) 5 μm , and (c) 0.9 μm . (d) SEM image of 900 nm patterned PEDOT-MA on substrate. (e) Diffraction from the film of part c. (f) Transmittance of the PET (black), PEDOT-MA-coated PET (magenta), and 0.9 μm line patterned PEDOT-MA on PET at different dose.

chain methacrylic groups may change the conduction channels and interpolymer interactions. A photoinduced conductivity change was also observed in the PEDOT films that were functionalized with carboxylic acid side chains.²⁵

The conductivity change of the PEDOT-MA from photoirradiation is much larger than that of the photo-cross-linkable PEDOT with a longer side chain (PEDOT-EMA)¹⁴ or PEDOT terminated with acrylates.²⁶ This indicates that the conductivity change from the cross-linking is directly dependent on the distortion of the PEDOT main chain. When the cross-linking units are short, the twisting of the main chain should be severe so that the conductive channels are distorted, to lower the conductivity of the cross-linked area. The main chain of the PEDOT with a longer side chain (PEDOT-EMA) or PEDOT terminated with acrylates is much less influenced by the side-chain cross-linking, and thus its conductivity change is small or negligible.^{14,26}

Photopatterning of PEDOT-MA. This pattern strategy (in combination with simple mask fabrication) can be applied in straightforward photopatterning to create defect-free patterns with at least submicrometer resolution. For photopatterning experiments, a 40 nm thick film was used. The PEDOT-MA film produced using VPP was exposed through a photomask. Figure 5a,b,c shows the patterns generated from photomasks with line widths of (i) 50, (ii) 5, and (iii) 0.9 μm , in which the light-exposed areas appeared to be bleached. In the line pattern with a spacing of 0.9 μm , the UV-exposed area appeared to be bleached and conglomerated flocks because of the cross-linking (Figure 5d). The cross-linking reaction was extended to the shaded interface and thus limited the pattern size up to 0.9 μm through the photomask technique. Nevertheless, these patterns were stable under ambient conditions.

When the line spacing of the patterns was $< 5 \mu\text{m}$, the patterned film became diffractive. In particular, the conductive line pattern with the spacing of $0.9 \mu\text{m}$ showed high diffraction that could be detected by the naked eye (Figure 5e). The diffraction efficiency of the film was determined to be 41% by the holographic set up equipped with a 491 nm laser.²⁷ Importantly, the diffractive film on PET was conductive. The σ_{RT} values of the diffractive film with $0.9 \mu\text{m}$ line spacing were 8.91, 1.34, and 0.93 S/cm when patterned under the light dose of 7.83, 15.6, and 90 J/cm^2 , respectively. Interestingly, after photopatterning, the transmittance of the patterned polymer films with the 900 nm patterns increased up to 75% because of bleaching of the PEDOT-MA from the photoreaction on the methacrylate functional group (Figure 5f). Therefore, the line patterned film with $0.9 \mu\text{m}$ spacing provided the first example of a diffractive CP film, which exhibits both flexibility and transparency. The simple photopatterning of the PEDOT-MA film can be used for diffractive conductive films, flexible electrode, and integrated organic circuits.

Conclusions

In conclusion, we demonstrated that films of PEDOT bearing side-chain methacrylates were prepared using VPP. The new CP film on PET film had a σ_{RT} of 30 S/cm , which decreased $< 10\%$ for a bending angle up to 80° . Submicron patterns were generated from the PEDOT-MA films by UV exposure. The line-patterned film with $0.9 \mu\text{m}$ spacing provided the first example of diffraction from a flexible, conductive, and transparent film. This constitutes an important step toward the patterning of conductive film to create high-contrast patterns with high flexibility, which are useful in optoelectronic devices, including flexible electrochromic, integrated circuit, electrochemical light-emitting, and solar cells.

Acknowledgment. We acknowledge the financial support of Seoul R&BD Program (10816) and the National Research Foundation (NRF) grant funded by the Korea government (MEST) through the Active Polymer Center for Pattern Integration (no. R11-2007-050-00000-0).

Supporting Information Available: FT-IR data of PEDOT and AFM images of PEDOT-MA on PET film before and after bending. This information is available free of charge via the Internet at <http://pubs.acs.org/>

References and Notes

- (1) Tehrani, P.; Hennerdal, L.; Dyer, A. L.; Reynolds, J.; Berggren, M. *J. Mater. Chem.* **2009**, *19*, 1799–1802.
- (2) (a) Sirringhaus, H.; Tessler, N.; Friend, R. H. *Science* **1998**, *280*, 1741–1744. (b) You, J.; Heo, J. S.; Lee, J.; Kim, H. S.; Kim, H. O.; Kim, E. *Macromolecules* **2009**, *42*, 3326–3332.
- (3) Kirchmeyer, S.; Reuter, K. *J. Mater. Chem.* **2005**, *15*, 2077–2088.
- (4) Guimard, N. K.; Gomez, N.; Schmidt, C. E. *Prog. Polym. Sci.* **2007**, *32*, 876–921.
- (5) Nie, Z.; Kumacheva, E. *Nat. Mater.* **2008**, *7*, 277–290.
- (6) Abdou, M. S. A.; Xie, Z. W.; Leung, A.; Holdcroft, S. *Synth. Met.* **1992**, *52*, 159–170.
- (7) (a) Abdou, M. S. A.; Holdcroft, S. *Macromolecules* **1993**, *26*, 2954–2962. (b) Abdou, M. S. A.; Arroyo, M. I.; Diaz-Quijada, G.; Holdcroft, S. *Chem. Mater.* **1991**, *3*, 1003–1006.
- (8) Persson, S. H. M.; Dyreklev, P.; Inganäs, O. *Adv. Mater.* **1996**, *8*, 405–408.
- (9) Lowe, J.; Holdcroft, S. *Macromolecules* **1995**, *28*, 4608–4616.
- (10) Chittibabu, K. G.; Li, L.; Kamath, M.; Kummar, J.; Tripathy, S. K. *Chem. Mater.* **1994**, *6*, 475–480.
- (11) Cai, S. X.; Keana, J. F. W.; Nabity, J. C.; Wybourne, M. N. *J. Mol. Electron.* **1991**, *7*, 63–68.
- (12) (a) Lowe, J.; Holdcroft, S. *Synth. Met.* **1997**, *85*, 1427–1430. (b) Yu, J. F.; Abley, M.; Yang, C.; Holdcroft, S. *Chem. Commun.* **1998**, 1503–1504.
- (13) Schanze, K. S.; Bergstedt, T. S.; Hauser, B. T. *Adv. Mater.* **1996**, *8*, 531–534.
- (14) Kim, J.; Kim, Y.; Kim, E. *Macromol. Res.* **2009**, *17*, 791–796.
- (15) (a) Winther-Jensen, B.; West, K. *Macromolecules* **2004**, *37*, 4538–4543. (b) Truong, T. L.; Luong, N. D.; Nam, J.; Lee, Y.; Choi, H. R.; Koo, J. C.; Nguyen, H. N. *Macromol. Res.* **2007**, *15*, 465–468.
- (16) (a) Segura, J. L.; Gómez, R.; Blanco, R.; Reinold, E.; Bäuerle, P. *Chem. Mater.* **2006**, *18*, 2834–2847. (b) Reeves, B. D.; Unur, E.; Ananthakrishnan, N.; Reynolds, J. *Macromolecules* **2007**, *40*, 5344–5352.
- (17) Zhang, D.; Ryu, K.; Liu, X.; Polikarpov, E.; Ly, J.; Tompson, M.; Zhou, C. *Nano Lett.* **2006**, *6*, 1880–1886.
- (18) Zhinong, Y.; Yuqiong, L.; Fan, X.; Zhiwei, Z.; Wei, X. *Thin Solid Films* **2009**, *517*, 5395–5398.
- (19) Garreau, S.; Louarn, G.; Bruissin, J. P.; Lefrant, S. *Macromolecules* **1999**, *32*, 6807–6812.
- (20) Reddy, B. S. R.; Balasubramanian, S. *Eur. Polym. J.* **2002**, *38*, 803–813.
- (21) Kvarnström, C.; Neugebauer, H.; Blomquist, S.; Ahonen, H. J.; Kankare, J.; Ivaska, A. *Electrochim. Acta* **1999**, *44*, 2739–2750.
- (22) Hernandez, V.; Ramirez, F. J.; Otero, T. F.; Navarrete, J. T. L. *J. Chem. Phys.* **1994**, *100*, 114–129.
- (23) Schanze, K. S.; Bergstedt, T. S.; Hauser, B. T.; Cavaleiro, C. S. P. *Langmuir* **2000**, *16*, 795–810.
- (24) Im, S. G.; Gleason, K. K. *Macromolecules* **2007**, *40*, 6552–6556.
- (25) Ali, E. M.; Kantchev, E. A. B.; Yu, H.-h.; Ying, J. Y. *Macromolecules* **2007**, *40*, 6025–6027.
- (26) Nielsen, C. B.; Angerhofer, A.; Abboud, K. A.; Reynolds, J. R. *J. Am. Chem. Soc.* **2008**, *130*, 9734–9746.
- (27) Kim, J.; Oh, H.; Kim, E. *J. Mater. Chem.* **2008**, *18*, 4762–4768.